Journal of Sound and Vibration 329 (2010) 4689–4704

Contents lists available at ScienceDirect

Journal of Sound and Vibration

journal homepage: www.elsevier.com/locate/jsvi

The design of an optimal viscous damper for a bridge stay cable using energy-based approach

Shaohong Cheng*, Neda Darivandi, Faouzi Ghrib

Department of Civil and Environmental Engineering, University of Windsor, 401 Sunset Avenue, Windsor, Ontario, Canada N9B 3P4

ARTICLE INFO

Article history:
Received 16 February 2009
Received in revised form
19 April 2010
Accepted 26 May 2010
Handling Editor: A.V. Metrikine
Available online 23 June 2010

ABSTRACT

An energy-based method is developed in the present paper to evaluate the damping property of a stay cable when transversely attached to a viscous damper. The overall increase of the cable damping offered by the external damper is determined by examining the time history of the kinetic energy in the damped cable. The concept of kinetic energy decay ratio is introduced as a key index to evaluate the effectiveness of a damper design in suppressing cable vibration. Compared to earlier studies, the proposed energy-based approach has no restrictions on the damper location. In addition, the flexural rigidity and sag extensibility of the cable are included in the formulation. Numerical simulation of free vibration of a damped stay cable is conducted using ABAQUS. To assist the design process, a set of damping estimation curves, which directly relate a damper design with the corresponding equivalent structural damping in a damped cable are developed for the practical parameter ranges of bridge stay cables. A number of numerical examples are presented. The validity and accuracy of the proposed method and damping estimation curves are verified by comparing with other studies. Results show that the energy-based approach developed in the present study is effective and efficient in determining the overall damping property of a cable-damper system, particularly in the preliminary stage of a damper design. In addition, the flexible applications of the developed damping estimation curves to damper design are demonstrated through these examples.

1. Introduction

Due to their low intrinsic damping and flexible nature, cables are often sensitive to dynamic excitations by various sources. Typically, in the case of stay cables on cable-stayed bridges, with the increased popularity of this type of bridges in the medium to long-span ranges and more matured field monitoring programs, many unfavourable cable vibration incidences were observed and reported from bridge sites in recent years, most of which relates to the excitation by wind or a combination of wind and rain (e.g. [1–4]). Frequent and excessive cable vibrations would cause connection failure and accelerate the fatigue and corrosion process in steel stay cables. These would significantly shorten their lifespan and increase the maintenance costs of cable-stayed bridges. Therefore, an effective reduction of cable vibration is not only a pressing issue in retrofitting existing bridges, but also a serious challenge and essential design aspects when a new bridge is under planning.

* Corresponding author. Tel.: +1 519 2533000x2629; fax: +1 519 9713686.
E-mail address: shaohong@uwindsor.ca (S. Cheng).

0022-460X/$ - see front matter
doi:10.1016/j.jsv.2010.05.027

Nomenclature

A	amplitude
c	damping coefficient of viscous damper
d_n	nth modal kinetic energy decay ratio
D	cable diameter
$E_k(t)$	kinetic energy contained in a vibrating cable at time t
$(E_{ki,n})_{\max}$	maximum kinetic energy of a damped cable in the ith cycle of the nth mode
$E_{k,n}(t)$	nth modal kinetic energy of a damped cable at time t
h	horizontal component of an additional cable tension due to vibration
H	pretension in the cable
L	cable length
L_d	distance from the damper to the nearest cable end
m	cable mass per unit span
$q_n(t)$	generalized coordinator of cable transverse displacement
S_c	Scruton number
$S_{i,n}$	amount of nth modal kinetic energy contained in the first half of the ith cycle
t_i	time instant when the ith cycle of vibration starts
T_{dn}	damped vibration period of the nth mode
v	transverse displacement of cable due to vibration
v_0	initial transverse displacement of cable due to vibration
$\dot{v}_0$	initial transverse velocity of cable due to vibration
$w_n(x)$	shape function of cable transverse displacement
y	lateral displacement due to self-weight of the cable
α_n	phase angle
Γ_d	non-dimensional damper location
δ	damping ratio of a cable
$\delta_{1,\max}$	maximum possible equivalent first modal damping ratio of a damped cable
δ_n	nth modal damping ratio of a damped cable
ξ	non-dimensional bending stiffness parameter of a cable
ρ	air density
φ_n	phase angle
ψ	non-dimensional damping parameter of a damper
$\psi_{opt,1}$	optimum damper size for the first mode
ω_{Dn}	damped circular frequency of the nth mode
ω_n	undamped circular frequency of the nth mode

For aesthetic and practical reasons, external damper is most commonly used in field. Its effectiveness in suppressing cable vibration has been studied extensively in the past three decades. In majority of the previous studies, cable was idealized as a taut string by neglecting its sag and flexural rigidity. The free vibration of a taut string when transversely attached to a damper was then formulated mathematically as a complex eigenvalue problem. The solution to this problem was derived by a number of researchers. Carne [5] is considered as one of the pioneers to evaluate the damping property of such a taut string-damper system. When designing guy cables for supporting the mast of vertical axis wind turbines, he studied how to suppress its lateral vibration using external dampers by deriving an approximate numerical solution to the complex eigenvalue problem. The damping ratio of the first mode of the guy cable was given approximately as a function of the damper location and its damping coefficient. Kovacs [6] used a semi-empirical approach and for the first time, identified an existence of optimal damping in a taut string-damper system. This was subsequently confirmed by other researchers [7–10]. In particular, Pacheco et al. [9] proposed a universal estimation curve, which related the normalized modal damping ratio of a taut cable with the normalized damping coefficient of the attached damper. This universal curve, which was applicable to an external damper placed very close to cable end, greatly saved effort in designing a traditional cable vibration suppression means. Krenk [10] derived an analytical formula for Pacheco's universal curve, based on which, an asymptotic solution to the free vibration of a taut string-damper system was developed. Later, this asymptotic solution was further extended to inclined cables [11] and shallow cables [12].

By including cable sag and cable bending stiffness in the formulation, Mehrabi and Tabatabai [13] presented a solution to the cable-damper system based on the finite difference method. In the study, the location of the damper was restricted to be very close to the cable end. The effects of these two parameters on the modal damping ratio of a cable were examined using the real stay cable properties in a bridge stay cable database [14]. Results showed that the influence of sag is not significant for most real cables. However, by neglecting the cable bending stiffness, the dynamic behaviour of a stay cable would be distorted to some extent. In the parametric study conducted in a subsequent work [15], the dependence of damping ratio of a cable-damper system on the normalized cable bending stiffness was observed for certain range of cable flexural rigidity. The significance of these two parameters on the dynamic behaviour of cable-damper system was also addressed by Krenk and Nielsen [12], Krenk and Hogsberg [16], and more recently, in the analytical studies by Fujino and Hoang [17], and Hoang and Fujino [18].

Though in practice, due to the inclined layout of stay cables on cable-stayed bridges, an external damper directly attached to an inclined stay cable has to be placed very close to the cable-deck anchorage for installation; practitioners know that in such configuration, the additional damping provided by the damper to the cable will be limited, particularly for longer stay cables [19]. Other possible means to overcome this disadvantage have been explored. Attempts have been made to combine the use of cross-ties and external dampers, of which the damper is attached to the cable through cross-

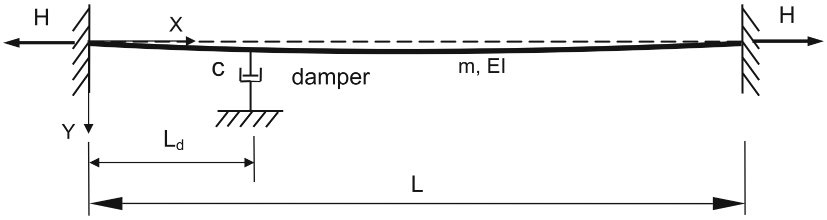

Fig. 1. Layout of a cable-damper system.

ties, so it could be installed at a location well beyond a few percent of cable length from cable-deck anchorage [4]. However, to the author's knowledge, only very few studies [20,21] lifted the restrictions on damper location in the formulation.

To improve the existing damper design techniques and shed light on developing novel alternative schemes with higher efficiency, a better comprehension and thorough understanding of the dynamic behaviour of a cable-damper system is essential. The present paper is focused on formulating and applying an energy-based finite element method to study how a specific damper design would affect the additional damping it could supply to an attached cable. To be more general, the proposed finite element model will take into account the bending stiffness and sagging effect of the cable. In addition, there will be no restriction on the damper location. The concept of kinetic energy decay ratio will be introduced as a key index to evaluate the effectiveness of a damper design in suppressing cable vibration. To assist design, a set of damping estimation curves will be proposed for the practical ranges of bridge stay cable parameters. These curves will relate a damper design directly with the equivalent structural damping of a damped cable. Empirical formulae for estimating optimum damper size and corresponding structural damping ratio will also be proposed, followed by a comparison with the existing ones derived based on taut string assumptions. Numerical examples will be presented to demonstrate the accuracy of the proposed methodology and flexible application of the damping estimation curves.

2. Formulation of the method

2.1. Important parameters in a cable-damper system

The cable-damper system under consideration is illustrated in Fig. 1. The cable is laid out in the horizontal direction with a chord length L, a pretension H, a mass per unit span m, and finite flexural rigidity EI. An external viscous damper is transversely attached to the cable at a distance L_d from one cable end, where $0 \leq L_d \leq L$. The damping coefficient of the viscous damper is denoted as c.

Compared to a single cable, the free vibration response of a cable, when attached to a transverse damper, highly depends on the magnitude of damper constant c. Considering two extreme cases of $c=0$ and $c=\infty$. If $c=0$, then the addition of damper has no effect on the dynamic behaviour of the cable, i.e. both natural frequencies and mode shapes remain the same as an undamped ones. Whereas if $c=\infty$, the damper will serve as a support. Therefore, the natural frequencies and mode shapes of the cable will be slightly modified. They will be equivalent to those of an undamped cable with span length of $(L-L_d)$. When $\infty < c < 0$, the cable will vibrate as a two-span structure connected at the damper location, with span lengths being L_d and $(L-L_d)$, respectively. In such a cable-damper system, the key parameters associated with the cable include its span length, unit mass, bending stiffness, sag extensibility ratio and pretension, while those associated with the damper include its location, damping coefficient and stiffness. In an earlier work [13], these main parameters were combined into non-dimensional forms as:

(a) Damper location parameter $\Gamma_d = L_d/L$. Majority of the previous studies have been restricted to cases, where $\Gamma_d \leq 0.06$.
(b) Cable bending stiffness parameter $\xi = L\sqrt{H/EI}$. According to the definition, it can be seen that the larger the cable non-dimensional bending stiffness parameter is, the more flexible the cable would be.
(c) Damping parameter $\psi = (\pi c)/(mL\omega_{1s})$, where $\omega_{1s} = (\pi/L)\sqrt{H/m}$ is the fundamental modal frequency of a taut string equivalent to the cable.

The definitions of these non-dimensional parameters will be used in the present study.

2.2. Kinetic energy decay ratio and its relation with an equivalent structural damping ratio

The energy contained in a vibrating cable includes the potential energy due to pretension, gravitational effect and the kinetic energy due to cable motion. If we take the static equilibrium position as the datum, when the cable passes at this position, the potential energy would be zero and the total energy is in the form of kinetic energy. Consequently, kinetic energy would reach its maxima and equal to the total energy in the cable at that moment. On the other hand, when the cable is at the largest vibration amplitude, the scenario is inverted and the total energy is in the potential form. For an

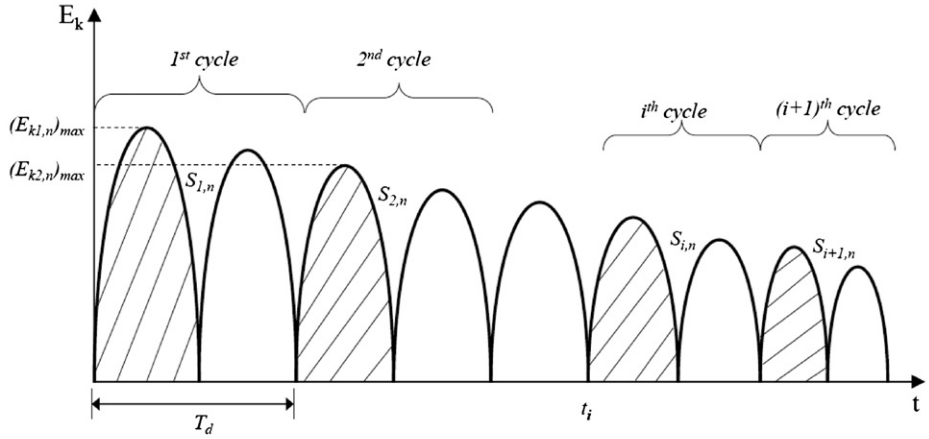

Fig. 2. Schematic illustration of kinetic energy time history of the *n*th mode of a damped cable.

undamped system, the total energy at any arbitrary time instant is a constant. However, with the presence of an external damper, the total energy, and thus the maximum kinetic energy and maximum potential energy would all be decaying functions of time. When evaluating a damper design for suppressing cable vibrations, how quickly it allows the dissipation of system energy and reduces cable motion to an acceptable level would be critical. In other words, the change in the system energy can be used to derive the amount of existing damping. To save the computation effort and owing to the fact that the amount of kinetic energy indicates directly the level of motion strength, instead of considering the changes of total system energy by summing up potential and kinetic energy, the time variation of maximum kinetic energy will be used to identify system damping.

For a typical cable-damper system shown in Fig. 1, free vibration of the cable can be initiated by displacing the cable a certain amount from the datum and then releasing suddenly. In general, such a dynamic response contains contributions of different modes with various significances. To determine the *n*th modal damping ratio, the cable needs to be excited in a way to allow the participation of the *n*th mode, preferably with relatively significant contribution in comparison to other existing modes. Then, the *n*th modal response will be extracted from the free vibration response data by applying appropriate filter for further analysis.

Fig. 2 illustrates schematically the kinetic energy time history of the cable when vibrating in the *n*th mode, where E_k denotes kinetic energy. Within a complete vibration cycle, the cable would pass the datum position twice; two local peaks can thus be observed from the kinetic energy time history in one cycle. The first local peak will be used to represent the maximum kinetic energy of the cable in that cycle. For example, $(E_{k1,n})_{\max}$ and $(E_{k2,n})_{\max}$ shown in Fig. 2 represents, respectively, the maximum kinetic energy of the cable in the first and the second cycle when vibrating in the *n*th mode. The difference, $(E_{k1,n})_{\max}-(E_{k2,n})_{\max}$, equals to the amount of energy dissipated through the damper within the first vibration cycle.

To be more general, when vibrating in the *n*th mode, the decreasing rate of maximum modal kinetic energy of a damped cable is defined as

$$d_n = \frac{1}{j}\sum_{i=1}^{j}\frac{(E_{ki,n})_{\max}-(E_{k(i+1),n})_{\max}}{(E_{ki,n})_{\max}} \tag{1}$$

where d_n is the *n*th modal kinetic energy decay ratio, $(E_{ki,n})_{\max}$ and $(E_{k(i+1),n})_{\max}$ are the maximum *n*th modal kinetic energy of the cable in the *i*th and the (*i*+1)th cycles, respectively, and *j* is the number of cycle pairs selected in the calculation. From Eq. (1), it can be seen that a larger d_n value corresponds to a higher kinetic energy dissipation. Therefore, when designing or evaluating the control schemes for a given cable, by introducing the same amount of 'initial energy,' the cable-damper system which yields the largest d_n will offer the fastest vibration mitigation solution for the *n*th mode.

For a convenient design formulation, the suppression effect provided by an external damper can be represented as an equivalent structural damping associated to the cable itself. Therefore, if a relationship between a particular external damper design and an equivalent structural damping can be established, it will greatly simplify the damper design process.

In the current study, the free vibration response of a cable-damper system is obtained from finite element simulation using ABAQUS (details will be presented in Section 3), from which, the kinetic energy time history of the studied system can be computed. Then, the kinetic energy decay ratio, and the corresponding equivalent structural damping ratio of the damped cable can be determined. The relation between kinetic energy decay ratio and an equivalent structural damping of a damped cable will be derived in this section based on a selected *n*th modal vibration response. It is worth to point out that though geometric nonlinearity of the cable-damper system has been considered in computing the kinetic energy time history in the numerical simulation, the representation of energy decay pattern in terms of an equivalent system damping is derived using an equivalent linear system. This strategy is commonly adopted for an initial design of nonlinear systems, where an equivalence between the original complex behaviour and a simplified linear system can be established.

Let us assume that the cable is set to vibrate in the nth mode. By using the separation of variables technique, the transverse displacement, v_n, due to cable vibration can be expressed as:

$$v_n(x,t) = w_n(x)q_n(t) \tag{2}$$

where $w_n(x)$ is the shape function which should be continuous and satisfies the geometric boundary conditions; and $q_n(t)$, the generalized coordinate, which in the case of linear systems has the form of

$$q_n(t) = A_n e^{-\delta_n \omega_n t}\cos(\omega_{Dn}t - \alpha_n) \tag{3}$$

where $A_n = \sqrt{q_0^2 + (\dot{q}_0 + q_0\delta_n\omega_n)^2/\omega_{Dn}^2}$ is the amplitude; $\alpha_n = \tan^{-1}[(\dot{q}_0 + q_0\delta_n\omega_n)/(\omega_{Dn}q_0)]$ is the phase angle; q_0 and $\dot{q}_0$ are the initial values of the generalized coordinate q_n and its first time derivative $\dot{q}_n$ at time t=0, respectively; δ_n is the nth modal damping ratio; ω_n and ω_{Dn} are the nth modal undamped and damped circular frequency, respectively. Consequently, the nth modal kinetic energy of a damped vibrating cable at an arbitrary time instant t is given by

$$E_{k,\,n}(t) = \int_0^L (m/2)\dot{v}_n^2(x,\,t)dx \tag{4}$$

Substitute Eqs. (2) and (3) into Eq. (4), yields

$$E_{k,n}(t) = \frac{mA_n^2}{2(\delta_n^2\omega_n^2 + \omega_{Dn}^2)} e^{-2\delta_n\omega_n t}\sin^2(\omega_{Dn}t - \alpha_n + \varphi_n)\int_0^L w_n^2(x)dx \tag{5}$$

where $\varphi_n = \tan^{-1}(\delta_n\omega_n/\omega_{Dn})$ is the phase angle. This clearly shows that the maximum kinetic energy in the nth modal vibration is decaying with time by

$$(E_{ki,n})_{\max} = (E_{k1,n})_{\max} e^{-2\delta_n\omega_n(i-1)T_{dn}} \tag{6}$$

where $(E_{k1,n})_{\max}$ and $(E_{ki,n})_{\max}$ are the maximum kinetic energy in the 1st and the ith cycle of the nth modal vibration, respectively; T_{dn} is the damped period of the nth mode. Based on Eq. (1), kinetic energy decay ratio of the nth mode can be determined by

$$d_n = \frac{1}{j}\sum_{i=1}^{j}\frac{(E_{ki,n})_{\max} - (E_{k(i+1),n})_{\max}}{(E_{ki,n})_{\max}} = 1 - e^{-2\delta_n\omega_n T_{dn}} \tag{7}$$

It can be seen from Eq. (7) that for a given linear system, the nth modal kinetic energy decay ratio is, as expected, a constant. This leads to a simple expression relating an equivalent structural damping of a damped cable with its kinetic energy decay ratio. The fact that $\omega_n T_{dn} \approx 2\pi$ yields

$$d_n = 1 - e^{-4\pi\delta_n} \tag{8}$$

or

$$\delta_n = -\ln(1 - d_n)/(4\pi) \tag{9}$$

2.3. *Refined formulation*

The methodology presented in Section 2.2, to determine the damping property of a cable-damper system based on the time variation of kinetic energy, can be applied to both numerical simulation and an experimental study. However, experimental data could be easily contaminated by noise, which would affect considerably the precision on locating the maximum kinetic energy within each vibration cycle, and thus the accuracy of the kinetic energy decay ratio and the equivalent structural damping ratio of the damped cable. On the other hand, although the response time history yielded from numerical simulation is “noise free,” if the time step is not properly selected, it would “miss” the instant when maximum kinetic energy actually occurs, and leads to similar problem of locating the true peak value.

To overcome these difficulties, a refined formulation is proposed, which, instead of comparing the maximum kinetic energy of the adjacent cycles, the difference between the total amount of kinetic energy contained in the first half cycle of the two adjacent vibration cycles i and $(i+1)$ are examined. They are represented by the shaded area $S_{i,n}$ and $S_{i+1,n}$ in Fig. 2. Similar strategy was used by Huang et al. [22] when proposing a new approach for assessing modal damping ratio of a linear structure based on free vibration response. In the refined formulation, the kinetic energy decay ratio is redefined as

$$d_n = \frac{1}{j}\sum_{i=1}^{j}\frac{S_{i,n} - S_{i+1,n}}{S_{i,n}} \tag{10}$$

where

$$S_{i,n} = \int_{t_i}^{t_i + T_{dn}/2} E_{k,n}(t)dt = \int_0^{T_{dn}/2} E_{k,n}(t + t_i)dt \tag{11}$$

$$S_{i+1,n} = \int_{t_i+T_{dn}}^{t_i+3T_{dn}/2} E_{k,n}(t)dt = \int_0^{T_{dn}/2} E_{k,n}(t+t_i+T_{dn})dt \tag{12}$$

where t_i is the time instant that the ith cycle of vibration starts. Substituting Eqs.(5), (11) and (12) into Eq. (10), yields the same result as Eq. (7), i.e. the nth modal kinetic energy decay ratio for a given cable-damper system is a constant. It is a function of the frequency, period, and damping ratio of the nth mode.

3. Numerical simulations

To determine the equivalent structural damping ratio in a cable-damper system using the proposed energy-based method, it is essential to know the time variation of kinetic energy in the damped cable, which, in the current study, is obtained by numerical simulation. A two-dimensional finite element model of a cable-damper system shown in Fig. 1 is developed using the general purpose nonlinear finite element software ABAQUS.

The B21 beam element in ABAQUS is selected to model the cable. This element considers the cable flexural rigidity in the formulation. It is developed based on the Timoshenko beam theory, which includes transverse shear deformation. It has two nodes, each with two translational and one rotational degree-of-freedoms. The large-strain formulation used for this beam element allows axial strains of arbitrary magnitude. The linear interpolation functions and a lumped mass formulation are used for this element. The pretension within the cable is simulated by introducing initial stress to the beam element along the axial direction as a static load. Fixed-end boundary condition is applied to both ends of the cable model.

To simulate the restriction on cable motion by the viscous damper, a DASHPOT1 element is selected. It is attached transversely to the cable model at one end and fixed at the other. This element applies a force to the cable which is linearly proportional to, but along the opposite direction of the cable velocity at the damper attaching point.

It is worth to note the nonlinear nature of the problem. For a cable-damper system in Fig. 1, given the cable has uniform cross section, the equation of motion describing its free vibration in vertical plane can be expressed as [15]

$$EI\frac{\partial^4 v}{\partial x^4} - H\frac{\partial^2 v}{\partial x^2} - h\frac{d^2 y}{dx^2} + c\frac{\partial v}{\partial t}\delta(x-L_d) + m\frac{\partial^2 v}{\partial t^2} = 0 \tag{13}$$

where v is the transverse displacement due to vibration; x is the coordinate along the chord; y is the lateral displacement due to self-weight of the cable, t is the time, $\delta(.)$ is the Dirac delta function; and h is the horizontal component of an additional cable tension due to vibration, which can be expressed as [13]

$$h = \frac{\int_0^L \frac{dy}{dx}\frac{\partial v}{\partial x}\,dx}{\int_0^L \frac{(ds/dx)^3}{EA}\,dx} \tag{14}$$

where $ds = \sqrt{dx^2 + dy^2}$ is the tangential length of an infinitesimal cable element. Since h depends on the deformed shape of the cable and varies with respect to time, it is a function of the cable true length at that time instant. The cable stiffness therefore needs to be updated at each time step of calculation. The finite element software ABAQUS used in the current study is capable to take care of this geometric nonlinearity issue by implementing the updated Lagrange kinematic formulation along the implicit direct integration during the simulation process.

In the numerical simulation, the static equilibrium profile of the cable under its self-weight and pretension is determined as the first step and set as datum, i.e. sag of the cable has been considered in the analysis. A displacement perturbation is then introduced at the cable mid-point and released suddenly. Free vibration response of the cable-damper system is computed by applying an implicit direct-integration approach in ABAQUS, of which an implicit unconditionally stable Hilber–Hughes–Taylor operator is used to integrate the equation of motion described by Eq. (13). The method uses the equilibrium conditions at time $t+\Delta t$ to determine the displacement response at the same instant. Filter is applied to the numerically obtained displacement time history to extract the first modal response. Based on the filtered data, the kinetic energy associated with the first mode at any specific time instant t can be computed according to Eq. (4). The kinetic energy decay ratio of the damped cable can then be determined either by Eq. (1) or (10), depending on if the selected time step in the numerical integration is fine enough to catch the maximum kinetic energy in each vibration cycle. Finally, the overall equivalent first modal damping ratio of the cable can be found by Eq. (9).

The present paper is focused on developing the relation between modal kinetic energy decay ratio of a damped cable vibrating in its first mode and an equivalent first modal damping ratio. Although more generally, vibration of a cable contains contributions from several different modes, it is pointed out [15] that effective control of the fundamental mode has the merit to improve damping in other modes and simplify the design process. Further, the same procedures proposed in this study can be readily extended to other modes for deriving such relation.

4. Comparison with other studies

Example 1. The proposed energy-based damping evaluation method and finite element model are verified using an experimental work by Tabatabai and Mehrabi [15] on a representative cable. The selected "representative" cable is based on the statistical evaluation from a database of over 1400 stay cables from 16 cable-stayed bridges [14]. Table 1 lists the properties of this model cable. A pretension of 122.1 kN is applied to the cable. The non-dimensional bending stiffness parameter of the cable is $\xi=100$.

In the reported test, a viscous damper was attached transversely to a horizontal cable at a location of 6% cable length to one cable end. The damper consists of a cylindrical container and a closely fit moving disk. Oils of various viscosity were

Table 1
Cable properties in the test by Tabatabai and Mehrabi [15].

Cable length	$L=13.695$ m
Equivalent axial rigidity	EA=49,138 kN (including grout and cover pipe)
Equivalent flexural rigidity	EI=2.28 kN-m^2 (including grout and cover pipe)
Bending stiffness parameter	$\xi=100$
Mass per unit length	m=3.6 kg/m

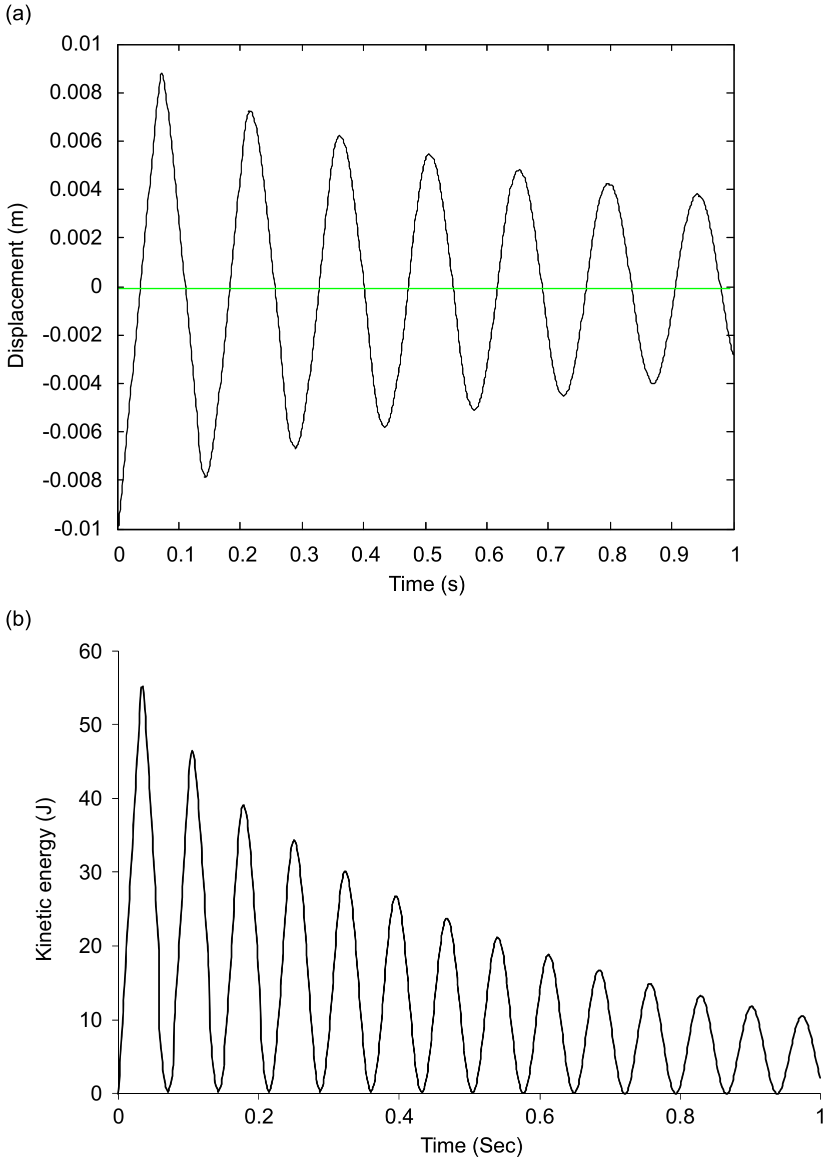

Fig. 3. Response of the damped cable in Example 1 (damping factor=1680 N s m^{-1}): (a) fraction of the displacement time-history at the middle point and (b) fraction of the kinetic energy time history.

filled in the cylinder to adjust the damper coefficient. The damper coefficients were taken as 1680 N s m^{-1} and 15,130 N s m^{-1}, for two separate tests. In each testing case, the cable was excited by applying a weight to its mid-point and then removed suddenly. The free vibration response of the cable mid-point was recorded using an accelerometer. The vibration response of first mode was obtained by filtering noise and higher modes of the recorded acceleration time histories. The damping ratio was determined by fitting an exponential curve to the peaks of the response time history. In addition, the damping ratio in these two cases was found by analytical solutions proposed by the same authors [15].

In the current study, the cable was numerically excited by introducing a displacement perturbation at the mid-point and then released suddenly. The time step used in the simulation is 0.0008 s. Compared to the fundamental period of the cable, which is 0.146 and 0.138 s, respectively, for damper coefficient of 1680 N s m^{-1} and 15,130 N s m^{-1}, the selected time step is approximately 0.5% of the first modal period. A low-pass filter of 7.5 Hz was applied to the numerically obtained dynamic response data to isolate the displacement time history of the first mode. Fig. 3(a) and (b) shows, respectively, a fraction of the filtered displacement time-history at the cable mid-point and a fraction of the first modal kinetic energy time history of the cable obtained from numerical simulation. The kinetic energy decay ratio was calculated by taking $j=6$ in Eq. (1). Based on Eq. (9), the equivalent first modal damping ratio of the cable is determined. The results of the current study and those by Ref. [15] are presented in Table 2 for comparison. Good agreement between results from these two studies can be observed. The cable fundamental frequency from the current study is slightly higher, with a difference of 2.6% in Case 1 and 0.8% in Case 2; whereas an equivalent first modal damping ratio yielded from the proposed energy-based formulation is, respectively, 4.7% and 6.3% higher than Ref. [15] for these two cases.

Example 2. For a typical bridge stay cable which has a non-dimensional bending stiffness parameter of $\xi=200$, an external viscous damper is needed to suppress unfavourable vibration induced by wind, rain–wind and parametric excitation. Assuming that the non-dimensional damping parameter ψ of the damper could vary between 0 and 60, and the damper could be installed at a position within 6% of cable length to the anchorage, we propose to determine the maximum possible equivalent first modal damping ratio of the damped cable when the damper is installed at $\Gamma_d=0.02$, 0.04, and 0.06.

Table 2
Comparison of first modal damping ratio in Example 1.

Case	Damping factor c (N m s^{-1})	Damping parameter ψ	Fundamental frequency (Hz)		Equivalent first modal damping ratio δ_1		
			Ref. [15]	Current study	Ref. [15]		Current study
			Test	FEA	Test	Analytical	FEA
1	1680	2.5	7.028	6.849	2.4	2.0	2.1
2	15,130	22.8	7.320	7.255	1.2	1.5	1.6

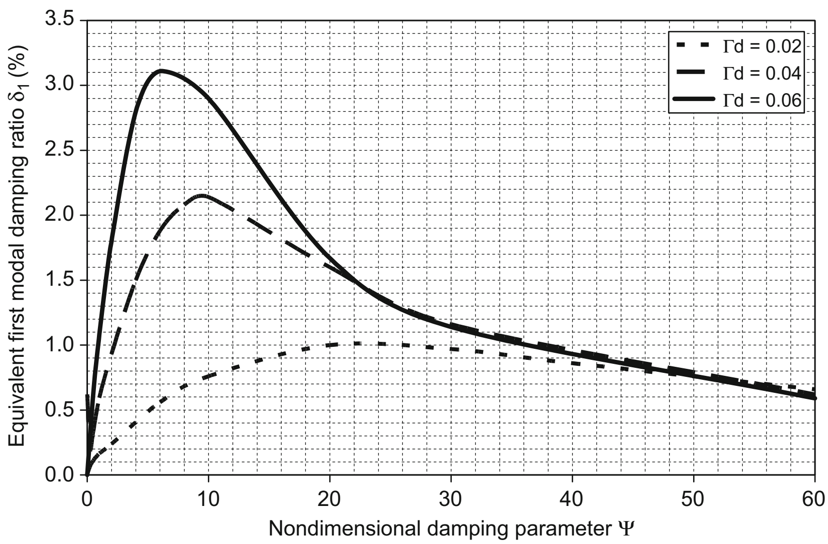

Fig. 4. Relation between damper size and cable equivalent first modal damping ratio in Example 2.

Numerical simulations of the first modal vibration of 18 cable-damper systems are conducted using different combinations of non-dimensional damping parameter ψ and damper location parameter Γ_d. The non-dimensional damping parameter, ψ, is taken equal to 10, 20, 30, 40, 50, and 60, and three typical values for Γ_d are selected namely 0.02, 0.04 and 0.06. The kinetic energy decay ratio of each system is found, which, based on Eq. (9), leads to an equivalent first modal damping ratio δ_1 of the system. Fig. 4 shows the relation between the damper size and the equivalent first modal damping ratio of the damped cable within the given range of ψ and Γ_d. Each curve in the figure corresponds to a specific damper location. As it can be seen from the figure, an optimum or maximum possible damping ratio exists at each damper location, which confirms the finding by some earlier studies [6–10], where several formulas are proposed for estimating the optimum damper size.

The formulas for estimating the optimum damper size and the corresponding damping ratio proposed by these studies are listed in Table 3. For comparison, the optimum damper size and damping ratio of the first mode obtained by the proposed energy-based method, and those based on the formulas in Table 3 are presented in Tables 4 and 5, respectively. It is observed that in the case of damper size, the current results are in good agreement with those by Tabatabai and Mehrabi [15], where the bending stiffness of the cable is considered in both studies. Interestingly, though in the studies by Kovacs [6], Yoneda and Maeda [7], Uno et al. [8], and Pacheco et al. [9], the cable is treated as a taut string, the results by the latter three are the least conservative, whereas the estimation by Kovacs [6] is the most conservative among all. As the damper moves further towards cable center, the impact of cable bending stiffness on the damper size diminishes. Nevertheless, the modal damping ratios obtained by different studies, as presented in Table 5, compare well. As indicated by Tabatabai and Mehrabi [15], if the bending stiffness parameter, ξ, is larger than 100, its effect on the modal damping ratio decreases.

Table 3
Formulas for estimating optimum damper size and corresponding damping ratio proposed by other studies.

Refs.	$\psi_{1,opt}$	$\delta_{1,\max}$
[6]	$0.5/\Gamma_d$	$0.5\Gamma_d$
[7]	$3.125\Gamma_d/\sin^2(\pi\Gamma_d)$	$6.25\Gamma_d(0.45+\Gamma_d)/(2\pi)$
[8]	$3.125\Gamma_d/\sin^2(\pi\Gamma_d)$	$3.3\Gamma_d/(2\pi)$
[9]	$0.1\pi/\Gamma_d$	$0.52\Gamma_d$
[15]	–	* $\frac{a\xi^b}{\psi^e_{1,opt}(\xi^b+d)}\ln\psi^e_{1,opt}$

* Parameters a, b, d, and e are given in Ref. [15].

Table 4
Comparison of optimum damper size $\psi_{1,opt}$ in Example 2.

Refs.	Γ_d=0.02	Γ_d=0.04	Γ_d=0.06
[6]	25	12.5	8.3
[7]	15.9	8.0	5.3
[8]	15.9	8.0	5.3
[9]	15.7	7.9	5.2
[15]	20	8.0	6.0
Present study	20	9.4	6.0

Table 5
Comparison of maximum damping ratio $\delta_{1,\max}$(%) in Example 2.

Refs.	Γ_d=0.02		Γ_d=0.04		Γ_d=0.06	
	$\delta_{1,\max}$ (%)	Difference (%)	$\delta_{1,\max}$ (%)	Difference (%)	$\delta_{1,\max}$ (%)	Difference (%)
[6]	1.00	0.0	2.00	6.5	3.00	3.5
[7]	0.94	6.0	1.95	8.9	3.04	2.3
[8]	1.05	−5.0	2.10	1.9	3.15	1.3
[9]	1.04	−4.0	2.08	2.8	3.12	0.3
[15]	1.05	−5.0	2.11	1.4	3.30	6.1
Present study	1.00	–	2.14	–	3.11	–

5. Design curves for estimating equivalent modal damping ratio

5.1. Damping estimation curves

When designing an external damper to control cable vibrations, it is critical to evaluate its effectiveness in suppressing unfavourable cable motion. Consequently, if a relation between the damper parameters and the corresponding cable equivalent structural damping ratio can be developed, the design process for selecting damper size and damper location could be greatly simplified. This type of relation will be particularly useful in the preliminary stage, where multiple design schemes need to be evaluated. A parametric study using the proposed energy-based method is conducted to develop a design procedure and a set of damping estimation curves for the cable-damper system. The ranges of the non-dimensional parameters ξ and ψ are selected based on a bridge stay cable database created by Tabatabai et al. [14]. The results are

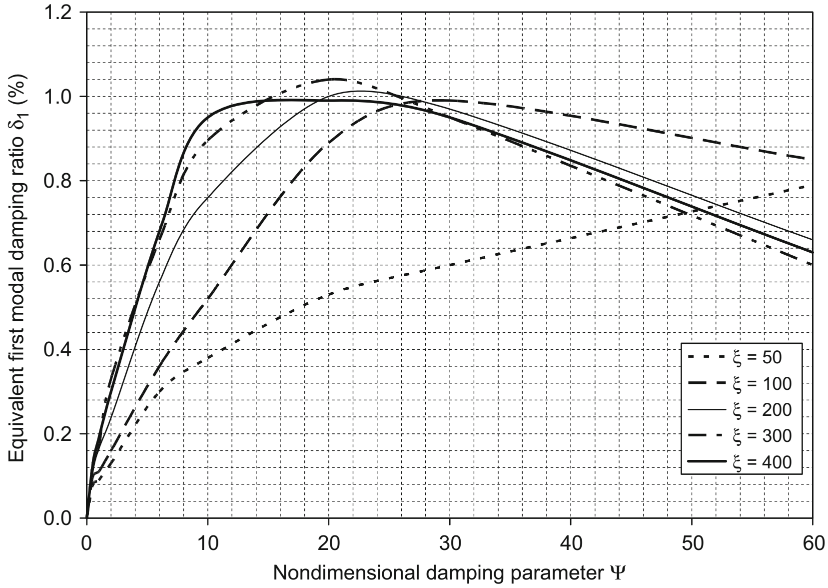

Fig. 5. Equivalent first modal damping ratio of a damped cable with a transverse viscous damper attached at Γ_d=0.02.

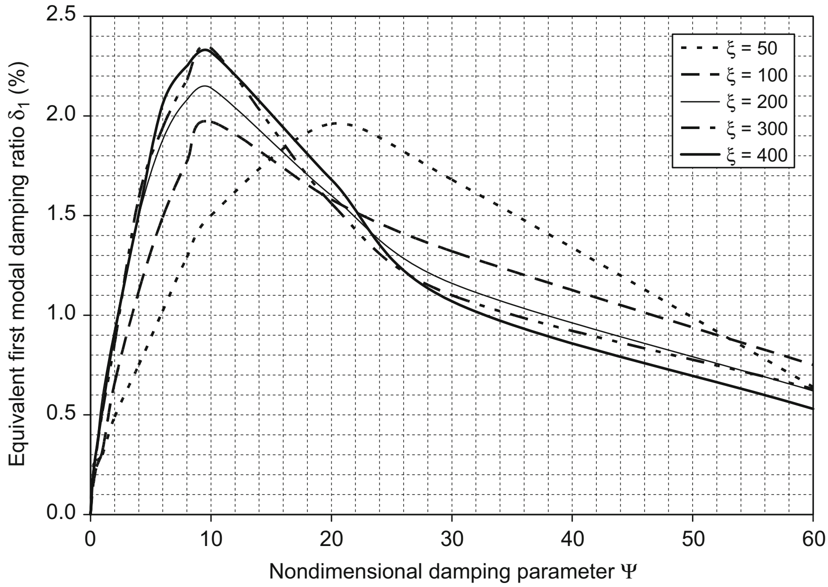

Fig. 6. Equivalent first modal damping ratio of a damped cable with a transverse viscous damper attached at Γ_d=0.04.

illustrated in Figs. 5–9. It is worth to note that the proposed design curves are developed by considering both the flexural rigidity and the sagging effect of the cable. Each of these figures portrays, for a specific damper location, the relationship between a damper size and an equivalent first modal damping ratio of the damped cable. Each curve is associated with a particular cable bending stiffness parameter ξ. Moreover, since the proposed method has no restrictions on damper location, besides the typical damper location of $\Gamma_d \leq 0.06$, which has been investigated by many of the earlier works, design curves at damper locations of Γ_d=0.10 and 0.15 are also presented. The extension to new damper locations has merit besides an academic illustration. It provides a reference for developing novel cable vibration controlling strategies at distances away from the cable anchorage, such as a hybrid system consisting of cross-ties and dampers [4]. The proposed energy-based method can be extended to derive similar design curves for $\Gamma_d > 0.15$. For the damper locations and the cable bending stiffness parameters in the ranges used in the present study, results show that a linear interpolation can be used to determine the damper size and the corresponding equivalent modal damping ratio.

As it can be observed from Figs. 5–9, optimum damper size exists at different damper locations. When a damper is placed very close to the cable anchorage, say, Γ_d=0.02, this optimum value is highly dependent on the flexural rigidity of

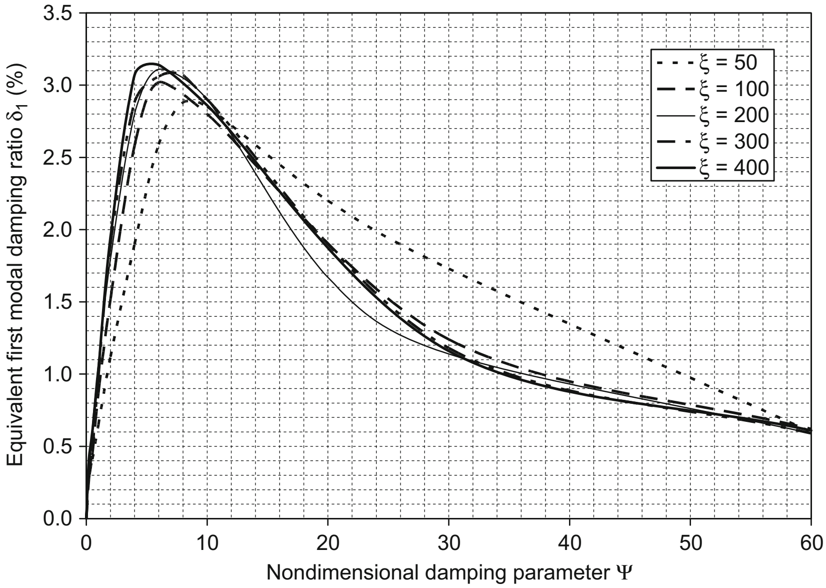

Fig. 7. Equivalent first modal damping ratio of a damped cable with a transverse viscous damper attached at Γ_d=0.06.

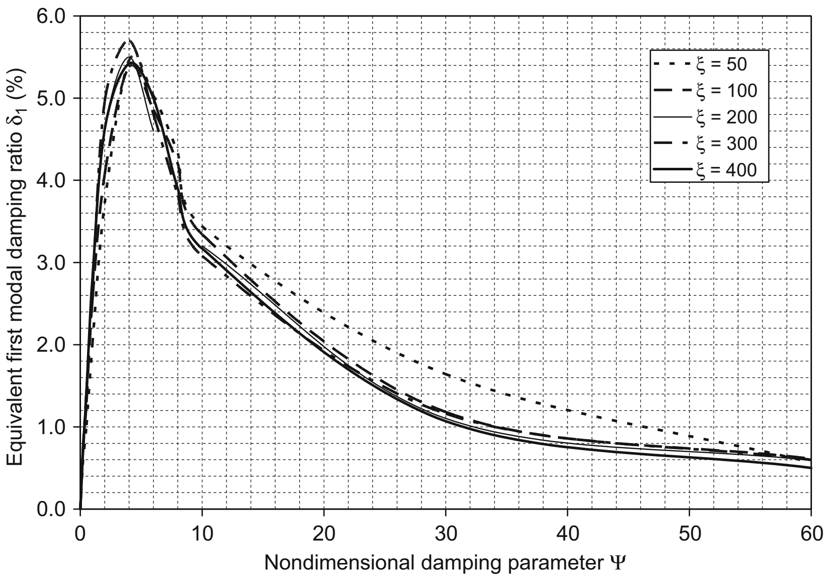

Fig. 8. Equivalent first modal damping ratio of a damped cable with a transverse viscous damper attached at Γ_d=0.10.

the cable. The stiffer the cable is (smaller ξ), the larger the optimum damper size will be. For example, if the cable becomes stiffer by decreasing its bending stiffness parameter ξ from 400 to 100, the optimum damping parameter $\psi_{opt,1}$ increases from 16 to 30. In the case of a very stiff cable with ξ=50, no optimum damping value has been identified for the range of damper size studied, i.e. $\psi_{opt,1} > 60$. However, as the damper moves further away from the cable anchorage, the optimum value becomes less sensitive to the cable bending stiffness. In particular, at Γ_d=0.10 and 0.15, regardless of the ξ value, all the $\delta_1 - \psi$ curves tend to collapse into one. There exists only one optimum damper size for those two damper locations, which is 4 for Γ_d=0.10 and 2 for Γ_d=0.15, respectively. Thus, should the damper be installed close to the cable end, the flexural rigidity of the cable must be considered in selecting optimum damper size.

Compared to a relatively flexible cable, to achieve the same suppression effect on a very stiff cable, say, ξ=50, a larger damper size is required when it is placed at $\Gamma_d \leq 0.06$. For example, to achieve an equivalent first modal damping ratio of 0.4%, for Γ_d=0.02, a damper with non-dimensional damping parameter ψ of 11.2, 6.7 and 4 is required for bending stiffness parameter ξ of 50, 100, and 200, respectively. This is due to the fact that for a stiffer cable, the attached damper would affect the motion of a longer cable segment; whereas for a flexible cable, the damper would only affect a shorter portion of the cable. Therefore, to be equally effective in controlling vibrations, a more “powerful” damper will be necessary for a stiffer cable.

In addition, as expected, it can be seen from Figs. 5 to 9 that for the same cable, the further the damper moves away from the cable end, the larger an equivalent damping ratio can be achieved. As indicated by Tabatabai and Mehrabi [15], the majority of the stay cables have a bending stiffness parameter $\xi \geq 150$. Therefore, for a typical stay cable which has ξ=300, when installing a damper at locations of Γ_d=0.02, 0.04, 0.06, 0.10 and 0.15, the corresponding maximum equivalent first modal damping ratio δ_1 would be 1.04%, 2.38%, 3.06%, 5.7%, and 7.7%, respectively.

5.2. Estimation of optimum damper size

Based on the damping estimation curves proposed in Figs. 5–9, the optimum damper size and the corresponding maximum structural damping ratio for the first mode of the cable at studied damper locations are summarized in Table 6. The bending stiffness parameter corresponding to the results in Table 6 varies depending on the damper location. It equals

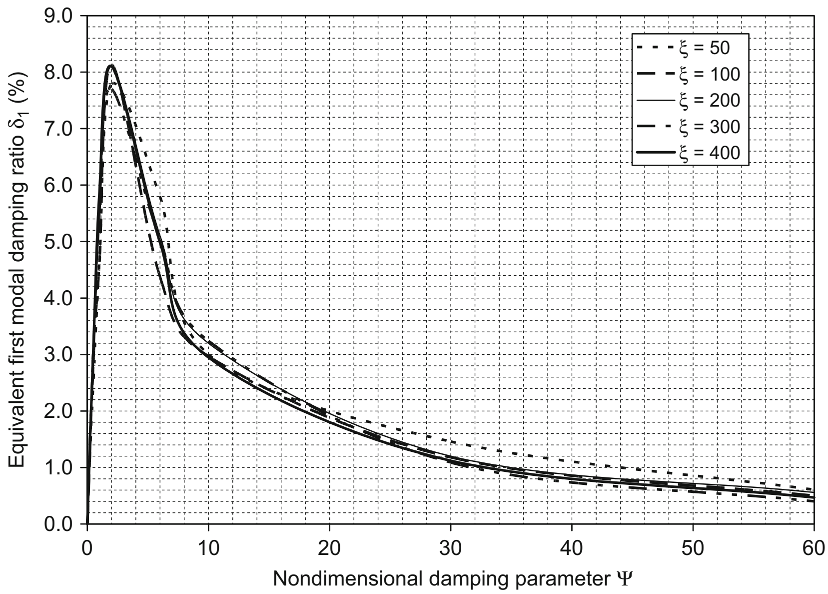

Fig. 9. Equivalent first modal damping ratio of a damped cable with a transverse viscous damper attached at Γ_d=0.15.

Table 6
Summary of optimum damper size and maximum equivalent structural damping ratio.

Γ_d	$\psi_{1,opt}$	$\delta_{1,\max}$(%)
0.02	20.0	1.04
0.04	9.5	2.38
0.06	5.5	3.15
0.10	4.0	5.70
0.15	2.0	8.10

to 300 when damper locates at 0.02, 0.04 and 0.10 L, and 400 at 0.06 and 0.15 L. This set of results provides an upper bound to show that within the practical parameter range of real stay cables, what would be the maximum achievable suppression effect at a specific damper location.

By applying regression analysis with a minimum coefficient of determination as 0.99, if both cable bending stiffness and damper location are included in the expression, the optimum damper size can be approximated by

$$\psi_{1,opt} = 0.261e^{-0.00061\xi}\boldsymbol{\Gamma}_d^{-1.192} \tag{14}$$

while the maximum equivalent structural damping ratio is given by

$$\delta_{1,\max} = 48.52\boldsymbol{\Gamma}_d^{1.03}\xi^{0.033} \tag{15}$$

In addition, for a more convenient comparison with some existing studies, of which the cable flexural rigidity is not included in the formulation, a simplified version of the above two expressions are found to be

$$\psi_{1,opt} = 0.271(\boldsymbol{\Gamma}_d)^{-1.10} \tag{16}$$

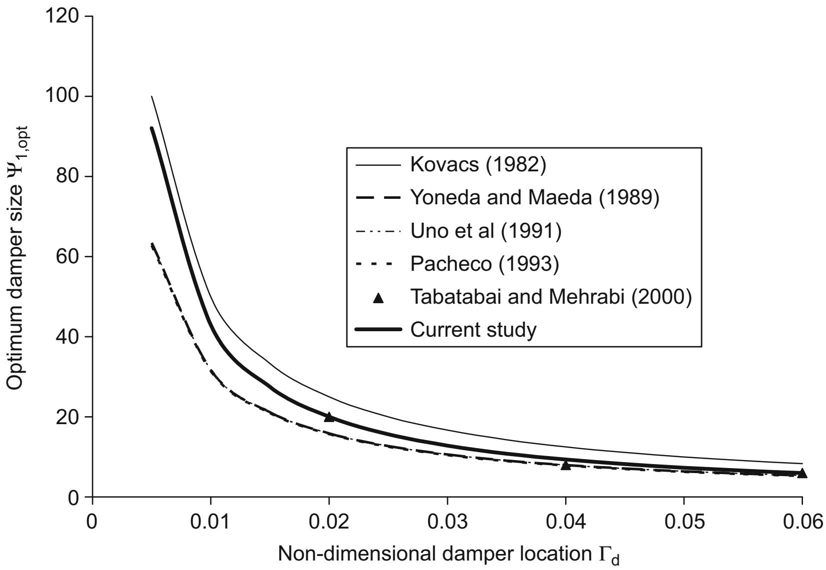

Fig. 10. Comparison of optimum damper size estimation.

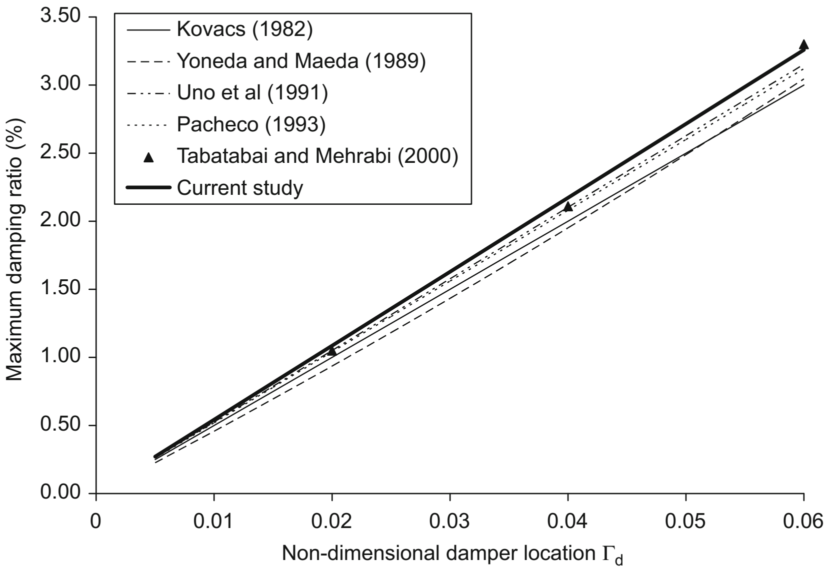

Fig. 11. Comparison of maximum equivalent structural damping ratio estimation.

$$\delta_{1,\max} = 0.543\boldsymbol{\Gamma}_d \tag{17}$$

Eqs. (16) and (17) are plotted in Figs. 10 and 11, respectively. For comparison, the relation curves proposed by earlier studies, listed in Table 3, are also shown in these two figures for the applicable range of $\Gamma_d \le 0.06$. It can be observed from Fig. 10 that by treating cable as a taut string, the estimated optimum damper sizes are divided into two branches, with those by Yoneda and Maeda [7], Uno et al. [8], and Pacheco [9] coincide with each other and at low end, while those by Kovacs [6] are more conservative. By considering the cable flexural rigidity in the formulation, the results by Tabatabi and Mehrabi [15] and the present study fall in between these two limits. In addition, as the damper moves away from the cable end, the estimated optimum damper size for a cable considering bending stiffness tends to agree with the lower branch. This again indicates that as the damper moves towards cable center, an impact of cable bending stiffness on the damper size decreases. The results in Fig. 11 suggest that similar to most of the earlier studies, the relation between the damper location and the maximum possible structural damping ratio is found to be approximately linear. Compared to the previous studies [6–9], of which the cable bending stiffness was excluded in the formulation, results given by the proposed energy-based method are found to be slightly higher. The difference becomes more obvious with the increase of damper location parameter Γ_d. This suggests that as the damper moves away from the cable end, the consideration of cable bending stiffness in the formulation will lead to a more optimum estimation of an equivalent damping ratio in the damper design.

5.3. Design examples

The design curves developed in the present study can be applied to the design of cable-damper systems in various ways. Numerical examples are presented in the following sections to illustrate the design procedure.

Example 3. Let us assume an external damper is to be designed for a stay cable to suppress vibrations induced by various dynamic sources. The properties of the cable are: length L=80 m, unit mass m=100 kg m^{-1}, diameter D=0.25 m, pretension H=5500 kN, equivalent bending stiffness (including grout and cover pipe) EI=1565 kN m^2. The damper is designed to have a damping coefficient c=586.3 × 10^3 N s m^{-1}, and placed at a distance equal to 5% of the cable length from the cable anchorage. We propose to determine an equivalent first modal damping ratio provided by an external damper.

Based on the given cable and damper properties, the non-dimensional parameters are

- cable bending stiffness parameter ξ=150
- damping parameter ψ=25
- damper location parameter Γ_d=0.05

From Fig. 6 (Γ_d=0.04), when ψ=25, an equivalent first modal damping ratio δ_1 of a cable with ξ=100 is 1.42%, whereas that for a cable with ξ=200 is 1.33%. Thus, by linear interpolation, when ξ=150, δ_1=1.38%. Similarly, based on Fig. 7 (Γ_d=0.06), it can be obtained that for ψ=25 and ξ=150, δ_1=1.42%. Therefore, linear interpolation between Figs. 6 and 7 yields that for a cable with ξ=150, if a damper with size ψ=25 is transversely attached to it at Γ_d=0.05, it will raise the first modal damping ratio of the cable to δ_1=1.40%.

In addition, by applying Eqs. (14) and (15), it can be found that for the cable described in the current example, if the damper location has to be set at Γ_d=0.05, then the optimum damper size should be $\psi_{1,opt}$=8.47. This would yield a maximum equivalent first modal damping ratio of 2.62%. Apparently, the proposed damper design in the example will not be the best choice.

Example 4. For the stay cable studied in Example 3, if the damper is installed at Γ_d=0.03, we can determine the minimum required damper size in order to prevent rain–wind induced vibration.

Post-Tensioning Institute (PTI) [23] recommends that to avoid rain–wind induced vibrations, the Scruton number S_c should satisfy the following relation, i.e.

$$S_c = \frac{m\delta}{\rho D^2} > 10 \tag{18}$$

where m is the cable unit mass, δ is the damping ratio of the cable, ρ is the air density, and D is the cable diameter. Eq. (18) can be rewritten as

$$\delta > \frac{10\rho D^2}{m} \tag{19}$$

Using the cable properties in Example 3 and assume that the air density ρ=1.29 kg m^{-3}, yields $\delta > 0.81\%$. Thus, a damper which could raise the equivalent damping ratio of the cable to at least 0.81% is necessary for suppressing rain–wind induced vibration.

Applying linear interpolation to estimate the damping from Figs. 5 and 6, we obtain that to provide 0.81% of an equivalent damping ratio, a damper should satisfy ψ=14.96 if installed at Γ_d=0.02, or ψ=2.15 if installed at Γ_d=0.04. Thus, for the given damper location of Γ_d=0.03 in this example, it corresponds to ψ=8.56.

Noting that the definition of the damping parameter $\psi=(\pi c)/(mL\omega_{1s})$, where $\omega_{1s}=(\pi/L)\sqrt{H/m}$ is the fundamental modal frequency of a taut string equivalent to the cable, the damping coefficient of the required damper would be

$$c=\psi\sqrt{Hm}=8.56\times\sqrt{5500\times10^3\times10^2}=200.75\times10^3\,\mathrm{kN\,s\,m^{-1}}$$

Therefore, to prevent rain–wind induced vibration, a damper with a least damping coefficient of c=200.75 × 10^3 kN s m^{-1} is needed to be installed 2.4 m from the cable-deck anchorage.

Example 5. For the same cable discussed in Examples 3 and 4, if a damper size corresponding to ψ=10 is selected for suppressing rain–wind induced vibration, we are interested at determining the least distance from the cable anchorage to the damper location.

As determined in Example 4, to prevent the rain–wind induced vibration on this particular cable (ξ=150), the minimum required overall structural damping ratio of the cable is 0.81%. Based on Figs. 5 and 6, it can be obtained that for a cable with non-dimensional bending stiffness of ξ=150, when attached to a damper of ψ=10 at Γ_d=0.02 and Γ_d=0.04, it will lead to an equivalent damping ratio of 0.64% and 2.06%, respectively. By linear interpolation, for the equivalent damping ratio to be 0.81%, the non-dimensional damper location parameter should be Γ_d=0.0224. Therefore, to prevent potential occurrence of the rain–wind induced vibration on this cable, a damper of size ψ=10 should be installed at least 1.792 m away from the cable–deck anchorage.

Example 6. The properties of a stay cable are taken from [7]: total length L=215.11 m, unit mass m=98.6 kg m^{-1}, cross-sectional area 0.009 m^2, pretension H=3.69 × 10^6 N, bending stiffness parameter ξ=380. Due to restrictions of geometrical layout, an external damper has to be installed at Γ_d=0.0235. We propose to determine the maximum possible equivalent modal damping ratio of the first mode.

From Figs. 5 and 6, it can be obtained that at damper locations of Γ_d=0.02 and 0.04, the maximum possible first modal damping ratio $\delta_{1,\max}$=1.04 and 2.38, respectively. Using linear interpolation, at Γ_d=0.0235, the maximum first modal damping is $\delta_{1,\max}$=1.27. Table 7 compares the maximum possible damping ratio of this damped cable by using various relationships proposed in other studies. Results show that the maximum damping ratios obtained from different studies are in good agreement. As indicated by Tabatabai and Mehrabi [15], for the relatively soft cable (ξ=380) considered in this example, the effect of cable flexural rigidity is not expected to be significant.

6. Conclusions

An energy-based approach is developed in the present study to evaluate the damping property of a cable when it is attached transversely to a viscous damper. The proposed method examines the time history of the kinetic energy contained in the cable-damper system. The decreasing rate reflects the energy dissipation capacity provided by an external damper. The effectiveness of a damper design in mitigating cable vibration has been studied using the kinetic energy decay ratio as a key index. The solution of the dynamic equation of the system is obtained by a finite element model and takes into account, implicitly, the flexural rigidity and sagging effect of the cable. For the development of the solution, no restriction on the damper location is made. Numerical simulations on the free vibration of cable-damper systems have been performed using the commercial software ABAQUS. The current work presents a set of curves which relate directly the extra damping provided by a designed damper with an equivalent structural damping ratio in a damped cable for practical parameter ranges of bridge stay cables. The set of curves is particularly useful in the preliminary design stage, where a quick comparison among various design options is needed. A number of numerical examples have been presented. The proposed design procedure is compared with available methodologies. Within this comparison, not only the accuracy and validity of the proposed energy-based approach and numerical model have been verified, but also the flexible application of the developed damping estimation curves has been demonstrated. In addition, it has been found that the bending

Table 7
Comparison of maximum damping ratio in Example 6.

Refs.	$\delta_{1,\max}$
[6]	1.18
[7]	1.11
[8]	1.24
[9]	1.22
[15]	1.16
Present study	1.27

stiffness of the cable should be considered in selecting optimum damper size when the damper is placed very close to the cable end, typically, within 6% of cable length. To achieve the same suppression effect, a larger damper size is required for a stiffer cable. If a damper is attached at a location more towards the cable mid-point, the consideration of cable flexural stiffness would lead to a more optimum estimation on the vibration reduction capacity of a damper design.

Acknowledgements

The authors are grateful to Natural Sciences and Engineering Research Council of Canada (NSERC) for supporting this project.

Appendix A. Supplementary material

Supplementary data associated with this article can be found in the online version at doi:10.1016/j.jsv.2010.05.027.

References

[1] Y. Hikami, N. Shiraishi, Rain–wind induced vibration of cables in cable-stayed bridges, *Journal of Wind Engineering and Industrial Aerodynamics* 29 (1988) 409–418.
[2] P.A. Irwin, A. Nedim, N. Telang, Wind induced stay cable vibrations—a case study, *in: Proceedings of the Third International Symposium on Cable Aerodynamics* (1999) 171–176.
[3] J.A. Main, N.P. Jones, Evaluation of viscous dampers for stay-cable vibration mitigation, *Journal of Bridge Engineering ASCE* 6 (6) (2001) 385–397.
[4] H. Bosch, Review of bridge cable vibrations within the USA, in: Proceedings of the 2006 Wind Induced Vibration of Cable Stay Bridges Workshop (2006) (on CD-ROM).
[5] T.G. Carne, Guy cable design and damping for vertical axis wind turbines, Report no. SAND80-2669, Sandia National Laboratory, Albuquerque, N.M., (1981).
[6] I. Kovacs, Zur frage der seilschwingungen und der seildämpfung, *Bautechnik* 10 (1982) 325–332.
[7] M. Yoneda, K. Maeda, A study on practical estimation method for structural damping of stay cable with damper, *in: Proceedings of the Canada–Japan Workshop on Bridge Aerodynamics* (1989) 119–128.
[8] K. Uno, S. Kitagawa, J. Tsutsumi, A. Inoue, S. Nakaya, A simple method of designing cable vibration dampers of cable-stayed bridges, *Journal of Structural Engineering, Toyko* 37A (1991) 789–798.
[9] B.M. Pacheco, Y. Fujino, A. Sulekh, Estimation curve for modal damping in stay cables with viscous damper, *Journal of Structural Engineering ASCE* 119 (6) (1993) 1961–1979.
[10] S. Krenk, Vibrations of a taut cable with an external damper, *Journal of Applied Mechanics* 67 (2000) 772–776.
[11] C. Crémona, Courbe universelle pour le dimensionnement d' amortisseurs en pied de haubans, *Revue Française de Génie Civil* 1 (1) (1997) 137–159.
[12] S. Krenk, S.R.K. Nielsen, Vibrations of a shallow cable with a viscous damper, *in: Proceedings of the Royal Society of London Series A (Mathematical, Physical and Engineering Sciences* 458 (2018) (2002) 339–357.
[13] A. Mehrabi, H. Tabatabai, Unified finite difference formulation for free vibration of cables, *Journal of Structural Engineering* 124 (11) (1998) 1313–1322.
[14] H. Tabatabai, A.B. Mehrabi, B.J. Morgan and H.R. Lotfi, Non-destructive bridge evaluation technology: bridge stay cable condition assessment, report Prepared for Federal Highway Admin., Construction Technology Laboratories, Inc., Skokie, Ill (1998).
[15] H. Tabatabai, A. Mehrabi, Design of mechanical viscous dampers for stay cables, *Journal of Bridge Engineering ASCE* 5 (2) (2000) 114–123.
[16] S. Krenk, J.R. Hogsberg, Damping of cables by a transverse force, *Journal of Engineering Mechanics ASCE* 131 (4) (2005) 340–348.
[17] Y. Fujino, N. Hoang, Design formulas for damping of a stay cable with a damper, *Journal of Structural Engineering ASCE* 134 (2) (2008) 269–278.
[18] N. Hoang, Y. Fujino, Analytical study on bending effects in a stay cable with a damper, *Journal of Engineering Mechanics ASCE* 133 (11) (2007) 1241–1246.
[19] H. Yamada, Control of wind-induced cable vibrations from a viewpoint of the wind resistant design of cable-stayed bridges, in: Proceedings of the International Seminar on Cable Dynamics, Tokyo, Japan (1997) 129–138.
[20] J.A. Main, N.P. Jones, Free vibration of taut cable with attached damper, I: linear viscous damper, *Journal of Engineering Mechanics ASCE* 128 (10) (2002) 1062–1071.
[21] J.A. Main, N.P. Jones, Free vibration of taut cable with attached damper, II: nonlinear viscous damper, *Journal of Engineering Mechanics ASCE* 128 (10) (2002) 1072–1081.
[22] F.L. Huang, X.M. Wang, Z.Q. Chen, X.H. He, Y.Q. Ni, A new approach to identification of structural damping ratios, *Journal of Sound and Vibration* 303 (1–2) (2007) 144–153.
[23] PTI Publication, in: *Recommendations for Stay-Cable Design, Testing and Installation*, fourth ed., Post-Tensioning Institute, 2001 March.